Chapter 1: Introduction

Pleckstrin is the major protein kinase C (PKC) substrate in blood platelets. PKC phosphorylation of pleckstrin occurs during platelet activation, a process that gets triggered in response to vascular injury. Pleckstrin consists of three domains, two of which are the prototypic pleckstrin homology (PH) domains at the termini of the protein. PH domains are found in many signalling molecules and often play a role in binding to a sub-class of phospholipids, phosphoinositides, which act as second messengers during and after platelet activation. Within this framework, the structural NMR studies of this thesis are carried out.

In this chapter, the biological background of platelet signalling networks and PH domains is introduced and the open questions about the pleckstrin protein are described (section 1.1). Strategies how to obtain NMR structures of large and multi-domain proteins like pleckstrin are outlined in section 1.2, and the theoretical background of the method that is used in this thesis is described in detail. A brief outline of the aims of this thesis is presented in section 1.3.

1.1 Biological background

1.1.1 Haemostasis

Haemostasis is the process by which the body responds to vascular injury, closes wounds and limits the loss of blood. Since the 1960s, the soluble factors of the "waterfall cascade" are known as the primary agents of blood coagulation that successively activate each other by proteolytic processing. The final activated enzyme of the cascade is the protease thrombin that cleaves a propeptide off fibrinogen. Fibrin polymerises and gets cross-linked by factor XIIIa, resulting in a mesh-like structure. The factors of the coagulation cascade have received much attention by clinical researchers because of their implication in disease. For example, loss-of-function mutations in the gene for factor VIII cause haemophilia A, a sex-linked recessive disease that was prevalent in some royal

households. By contrast, defective control of blood coagulation – unwarranted blood clotting – leads to thrombosis, stroke and heart attack.

Besides the soluble factors of the coagulation cascade the blood platelet (thrombocyte) is the other crucial player in haemostasis. Deficiency or low numbers of platelets also give rise to a variety of disease, ranging from mild to severe bleeding disorders. The synergistic interaction between soluble factors, blood platelets and the endothelium provide the actual basis of haemostasis (Majerus, 2001).

1.1.2 Platelet physiology

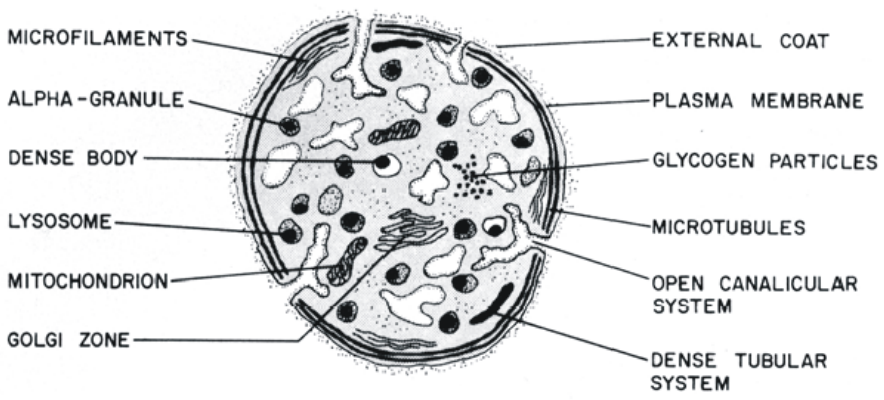

Figure 1.1: Platelet physiology. *A platelet cell is shown schematically, looking at a transverse section of the disc. Adapted from http://www.akh-wien.ac.at/biomed-research/htx/anatomy.htm*

Platelets are small anuclear cells that are derived from megakaryocyte stem cells in the bone marrow. They contain mitochondria and are able to perform basic metabolism and even protein synthesis to some extent. They only survive for 7 to 10 days in the circulation before they are cleared by the spleen. Fig. 1.1 shows a schematic illustration of a platelet cell. There are a large number of storage granules which are classified as α-granules and dense bodies. The former harbour polypeptides involved in coagulation and cell adhesion, as well as growth factors, whereas the latter are filled with small molecules such as ADP and serotonin. Resting platelets are smooth discs of about 2-3μm in diameter, reminiscent of red blood cells, but much smaller. The cytoskeleton forms a strong ring structure in the plane of the disc that maintains its shape. The plasma

membrane features a large number of invaginations called open the canalicular system that increase the surface area and/or provide storage capacity for membrane components (Majerus, 2001).

1.1.3 Formation of the haemostatic plug

During the physiological formation of a blood clot at the site of injury platelets proceed through the stages of adherence, activation, aggregation, secretion and contraction.

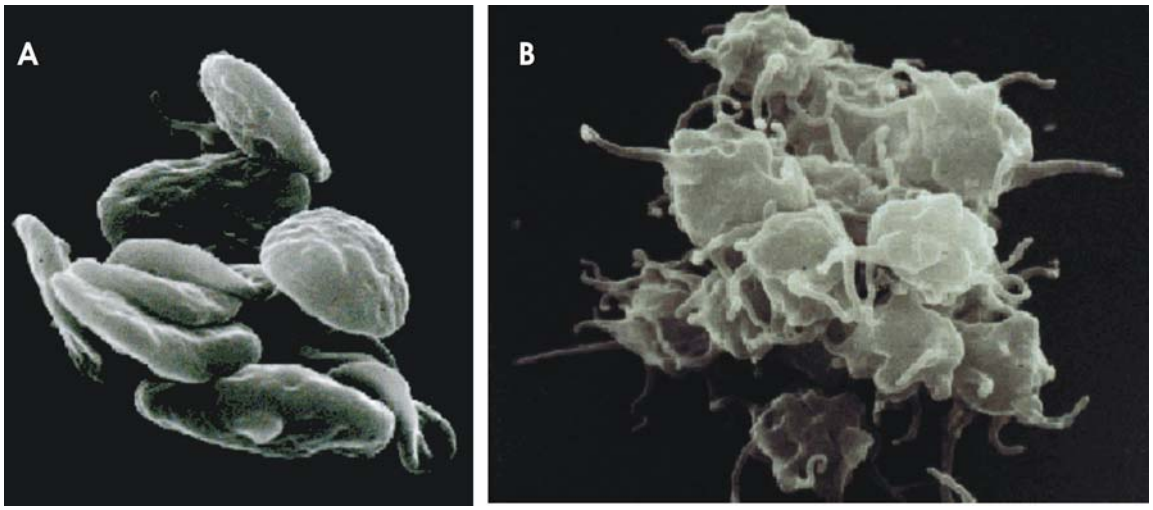

Figure 1.2: Scanning electron microscopy pictures of platelets. A: resting. B: activated. *Adapted from http://www.akh-wien.ac.at/biomed-research/htx/anatomy.htm*

Platelets possess surface receptors for markers of vascular injury, such as collagen, fibronectin and van Willebrand factor (vWF). Interactions between these receptors and their ligands make platelets adhere to the site of injury. Furthermore the adherent platelets become activated and spread over the wound surface. Activation involves dramatic shape changes; the cells become more spherical and membrane protrusions named lamellopodia and filopodia are formed that can extend to lengths of several diameters of a resting platelet (Fig. 1.2). This requires massive reorganisation of the cytoskeleton and actin polymerisation. The blood coagulation factor cascade is set off parallel to platelet activation. In fact, the platelet membrane binds activated factors and factor complexes. Thereby it accelerates the reactions and protects coagulation factors from inhibition and

degradation. In turn, thrombin that is produced locally recruits and activates additional platelets.

Platelet activation also results in sensitisation of surface integrins $\alpha_{IIb}\beta_3$ that become competent for binding to fibrinogen. Fibrinogen cross-links activated platelets, which leads to the formation of insoluble aggregates *in vitro*. Hence this process is called platelet aggregation. Aggregation can be measured as changes in optical density. This fundamental assay has been used extensively to characterise many aspects of platelet biochemistry. Activation and aggregation are accompanied by secretion of storage granules. The release of clotting factors and platelet agonists serves to accelerate activation and aggregation. Furthermore, wound healing is promoted by PGDF (platelet derived growth factor) and blood loss is minimised by vasoconstrictors (thromboxane A_2). Finally, platelets retract their membrane protrusions by the action of their acto-myosin motor. Since the fibrin receptors (integrins) are attached to the actin cytoskeleton the whole clot structure contracts and hardens. Thus, the mature clot is formed (Majerus, 2001).

1.1.4 Signalling pathways in platelets

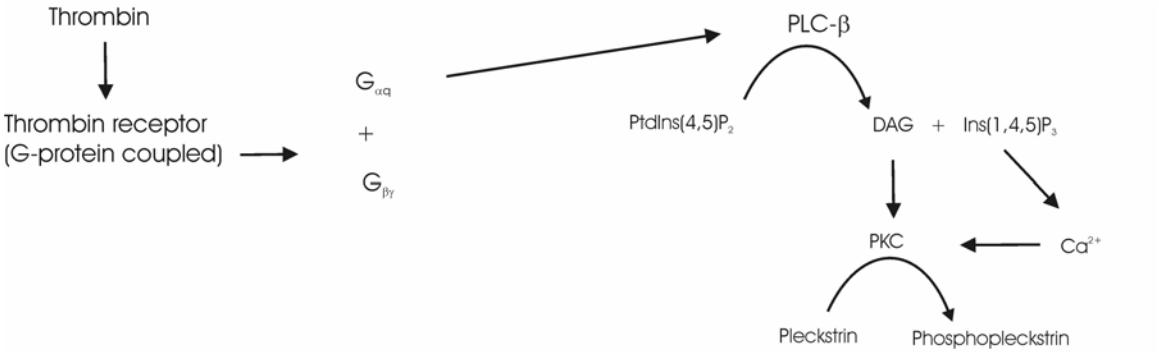

Figure 1.3: The principal signalling pathway in platelets leading to pleckstrin phosphorylation.

Platelets are activated by a number of agonists (thrombin, collagen, ADP, etc) that bind to their dedicated receptors. Thrombin is the most potent activator and binding to its G-protein coupled receptor liberates the associated α subunit, $G_{\alpha q}$, from its trimeric complex. G_{aq} activates phospholipase C-β (PLC-β), an enzyme that hydrolyses

phosphatidylinositol-4,5-bisphosphate (PtdIns(4,5)P_2) yielding the second messengers diacyl glycerol (DAG) and inositol-1,4,5-trisphosphate (Ins(1,4,5)P_3). DAG directly activates protein kinase C (PKC), while Ins(1,4,5)P_3 promotes the release of Ca^{2+} from internal stores. Ca^{2+} is involved in many processes, including granule secretion, myosin and PKC activation. Apart from the principal signalling pathway of PLC and PKC, other routes involving tyrosine protein kinases, small GTPases (Rho, Rac) and phosphatidylinositol-3-kinase (PI-3K) are activated. The latter produces the lipid second messengers phosphatidylinositol-3,4-bisphosphate (PtdIns(3,4)P_2) and phosphatidylinositol-3,4,5-trisphosphate (PtdIns(3,4,5)P_3) (Majerus, 2001; Offermanns, 2000).

1.1.5 Pleckstrin

When platelets are incubated with γ-^{32}P-ATP prior to activation with thrombin, a major phosphoprotein of 47kDa is observed (Lyons and Atherton, 1979). This protein is called p47 or pleckstrin (for platelet C-kinase substrate). Since the thrombin-PKC signalling pathway is the principal one in platelets, pleckstrin is thought to be of central importance for transmitting the thrombin stimulus. In clinical studies, pleckstrin is used as a molecular marker of early platelet activation.

The pleckstrin protein consists of three domains, two of which are the prototypic pleckstrin homology (PH) domains (Haslam et al., 1993). The two PH domains are located at the termini of the protein and are denoted N-PH and C-PH accordingly here (Fig. 1.4). The intervening sequence harbours a DEP (dishevelled, egl-1, pleckstrin) domain. The PKC phosphorylation sites have been mapped to the linker between N-PH and DEP – three in total (Abrams et al., 1995b). This linker is about 20 residues in length just as the linker between DEP and C-PH. Pleckstrin is only expressed in blood cells, however, a paralog (pleckstrin-2) is found in a greater variety of cell types (Hu et al., 1999).

It is assumed that phosphorylation converts pleckstrin into its active form and promotes association with the plasma membrane (Ma et al., 1997; Sloan et al., 2002). Despite the effort of several research groups, pleckstrin's precise function remains obscure. However, the data on pleckstrin that has accumulated over the years does provide some clues.

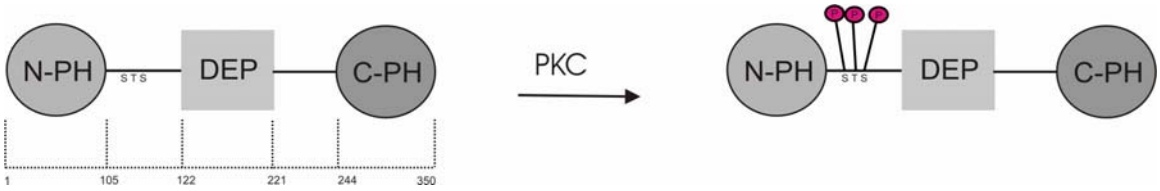

Figure 1.4: The pleckstrin molecule*. Domain boundaries are indicated. PKC phosphorylates three positions in the linker between N-PH and DEP.*

In platelets, phosphopleckstrin is found in a cytosolic complex with an inositolpolyphosphate-5-phosphatase (IPP-5-Pase) and stimulates phosphatase activity (Auethavekiat et al., 1997). This might serve to degrade Ins(1,4,5)P_3 and terminate the Ca^{2+} signal. Since pleckstrin is a highly expressed protein and in vast excess of IPP-5-Pase, there must be additional functions. Direct interactions between both N-PH and C-PH with Gβγ have been described (Abrams et al., 1996b), and pleckstrin has been also shown to inhibit PI-3Kγ involving interactions with Gβγ (Abrams et al., 1996a). Since the product of PI-3K, PtdIns(3,4,5)P_3 stimulates pleckstrin phosphorylation (Toker et al., 1995), this seems to indicate a function in down-regulating the pathway that leads to its own activation. Finally, pleckstrin is co-immunoprecipitated with a yet unidentified tyrosine phosphorylated protein of 30kDa and it interacts directly with this protein *in vitro* (Liu and Makowske, 1999). Thus, pleckstrin may be the agent of a negative feedback loop that down-regulates or even terminates the signalling pathways that lead to its own activation by sequestering Gβγ subunits of trimeric G-protein coupled receptors and by activation of IPP-5-Pase.

The possible role of pleckstrin in other haematopoietic cells has also been investigated: the antimicrobial response in neutrophils leads to pleckstrin phosphorylation and subsequent translocation to the membrane/cytoskeleton (Brumell et al., 1997). In macrophages, pleckstrin accumulates on phagosomal membranes even without the requirement for phosphorylation (Brumell et al., 1999). Experiments in natural killer cells show that phosphorylated pleckstrin translocates to the membrane (al-Aoukaty et al., 1999). Furthermore pleckstrin is co-immunoprecipitated with PI-3Kγ and Gβγ and vice versa. These findings confirm the results in platelets and indicate that the function in other blood cells might be comparable.

The most compelling evidence showing that pleckstrin has a function in cytoskeleton reorganisation and hence platelet activation is presented by Abrams' group. When expressed in cell lines where it is normally absent, such as cos-1 cells, pleckstrin is efficiently phosphorylated, localises to the plasma membrane and inhibits phospholipase C (Abrams et al., 1995a). Furthermore, pleckstrin transforms the morphology of cos-1 cells. Membrane ruffles form on the dorsal surface and the actin cytoskeleton is reorganised (Ma et al., 1997). These effects are dependent on phosphorylation and the presence of the N-terminal PH domain. Mutations in N-PH that abrogate phosphoinositide binding (see below) also destroy the ability of pleckstrin to induce the above changes. In similar experiments, it was shown that N-PH alone translocates to the membrane and is sufficient to cause the phenotype of the full-length molecule (Ma and Abrams, 1999).

Pleckstrin-induced actin rearrangements and membrane ruffling depend at least partially on Rac (Ma and Abrams, 1999). Moreover, cell spreading caused by pleckstrin in HEK293 cells depends on integrins (Roll et al., 2000). Spreading is only efficient on a surface coated with fibrinogen and requires a functional integrin β3 subunit. This subunit is also found in the platelet fibrinogen binding integrin. Again, N-PH is required and phosphorylation enhances the extent of spreading.

The experiments by Abrams' group show that pleckstrin is able to induce transformations of cell morphology concomitant with cytoskeletal rearrangement. It is assumed that pleckstrin also has an important role in cytoskeletal rearrangements during platelet activation; however, the down-stream targets of pleckstrin are still obscure.

Structural characterisation of pleckstrin N-PH (Yoon et al., 1994) and DEP (Civera et al., 2004) have provided important information on the possible function of these modules in the pleckstrin protein. Pleckstrin N-PH was the first PH domain to be biochemically and structurally characterised. It was shown to bind to vesicles containing PtdIns(4,5)P_2 suggesting that it may have a role in membrane anchoring (Harlan et al., 1994; Harlan et al., 1995). However, the relatively low affinity of this interaction raises the possibility that the biological target of N-PH is not primarily or exclusively a membrane lipid, but a protein. The results of the *in vivo* experiments (see above) which focus on the role of N-PH can be interpreted in favour of either the phosphoinositide or the protein hypothesis.

As for the DEP domain, its most striking feature is a highly charged β-hairpin with a conserved lysine residue at its tip. If this residue is mutated to methionine in the DEP domain of the *Drosophila* dishevelled protein, it causes planar polarity defects in eye development, probably by disrupting protein-protein contacts (Boutros et al., 1998).

Clearly, further studies are required to resolve the most important questions concerning pleckstrin's role in the platelet signalling network. From a structural point of view, two main questions await investigation: a) the structure of the uncharacterised C-terminal PH domain and b) the overall architecture of the pleckstrin protein and its regulation by PKC phosphorylation. Both questions are addressed in the work presented in this thesis.

1.1.6 Pleckstrin homology domains

PH domains are modular components of a great number of proteins that are predominantly involved in signalling. In the absence of a strict sequence homology (there is only one absolutely conserved residue) secondary and tertiary structure are remarkably conserved between all PH domains. The fold consists of a seven-stranded β-barrel (or β-sandwich) that is capped at one side by a C-terminal helix (Fig. 1.5). Opposite the helix is the so-called "open" side that consists of several loops that can be quite variable in length and composition. The structures of pleckstrin N-PH and β-spectrin PH were the first structures of PH domains to be solved, both by nuclear magnetic resonance (NMR) spectroscopy (Macias et al., 1994; Yoon et al., 1994). Soon thereafter, Fesik and co-workers showed that N-PH binds lipid vesicles containing PtdIns(4,5)P_2 and proposed a general function of PH domains in binding to this class of phospholipids and, by consequence, in membrane targeting (Harlan et al., 1994; Harlan et al., 1995). The binding site for the phosphoinositide ligand is at the open side of the domain. In fact, most PH domains have a strong positive electrostatic potential at the open side, which explains their affinity for strongly negatively charged ligands (Blomberg et al., 1999). When basic residues are mutated in the loops flanking the open side of the domain, phosphoinositide binding is lost, as demonstrated for N-PH (Harlan et al., 1995).

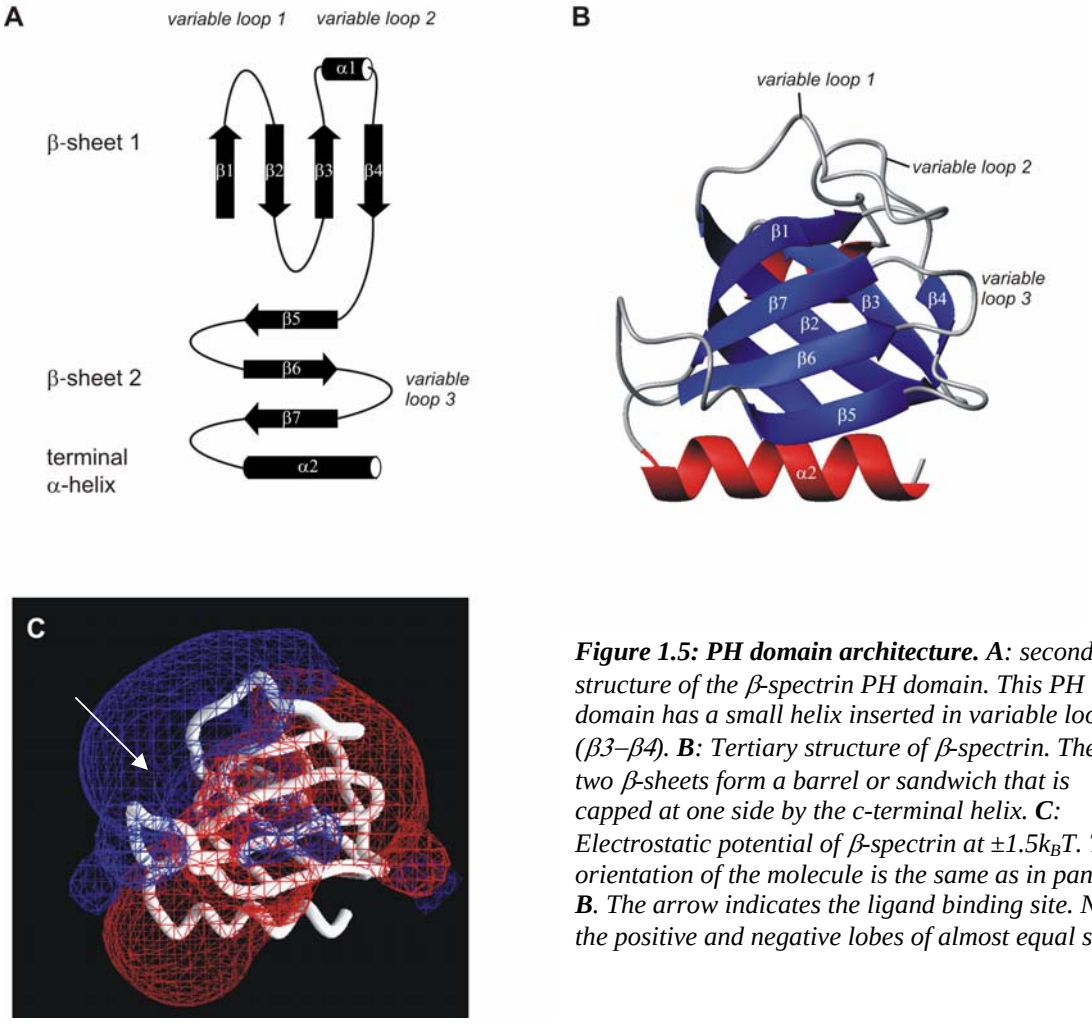

***Figure 1.5: PH domain architecture. A**: secondary structure of the β-spectrin PH domain. This PH domain has a small helix inserted in variable loop 2 (β3–β4). **B**: Tertiary structure of β-spectrin. The two β-sheets form a barrel or sandwich that is capped at one side by the c-terminal helix. **C**: Electrostatic potential of β-spectrin at ±1.5k_BT. The orientation of the molecule is the same as in panel **B**. The arrow indicates the ligand binding site. Note the positive and negative lobes of almost equal size.*

The ligand binding properties of PH domains have been investigated in detail. Almost every PH domain tested seems to be capable of binding to one or the other phosphoinositide, but many of these interactions are either promiscuous, weak, or both (Lemmon, 2003; Lemmon and Ferguson, 2001). Most likely, the aforementioned positive potential at the open side allows indiscriminate binding of negatively charged ligands *in vitro*. The relevance of weak and unspecific binding *in vivo* is problematic, yet it may have a regulatory or auxiliary function.

Rather than being a general function of the PH domain family, high affinity (i.e. K_D in the low micromolar or sub-micromolar range) phosphoinositide binding appears to be limited to a relatively small sub-group. For example, the PH domain of PLC-δ is highly selective for PtdIns(4,5)P_2 (Lemmon et al., 1995). Due to this property, the PLC-δ PH domain is

widely used as a sensor of PtdIns(4,5)P_2 (and Ins(1,4,5)P_3) in living cells (Balla and Varnai, 2002). Several PH domains with different specificities can be used for *in vivo* imaging and offer the possibility to monitor many aspects of phosphoinositide localisation and metabolism. Table 1.1 lists the most important representatives of the different ligand binding classes.

Phosphoinositide	***PH domain***	***Reference***
PtdIns(4,5)P_2	PLC-δ	(Lemmon et al., 1995)
PtdIns(3,4,5)P_3	Grp-1	(Kavran et al., 1998)
PtdIns(3,4,5)P_3 and PtdIns(3,4)P_2	PKB/Akt, DAPP1	(Dowler et al., 1999; Frech and Hemmings, 1998)
PtdIns(3,4)P_2	TAPP1	(Dowler et al., 2000)

Table 1.1: High-affinity PH domains and their phosphoinositide ligands. *Only the most important representatives are shown. All of these are used as biosensors for their ligand in living cells.*

The biochemical network of phosphoinositide metabolism is shown in Fig. 1.6. PtdIns(4,5)P_2 is the precursor of PtdIns(3,4,5)P_3. PtdIns(3,4)P_2 is produced by several pathways: 5-dephosphorylation of PtdIns(3,4,5)P_3 and phosphorylation of PtdIns(3)P and PtdIns(4)P by PI-4K and PI-3K, respectively. In resting cells, the levels of all phosphoinositides except PtdIns and PtdIns(4,5)P_2 are low. Therefore, all others may act as secondary messengers. In platelets, this is the case for both PtdIns(3,4)P_2 and PtdIns(3,4,5)P_3.

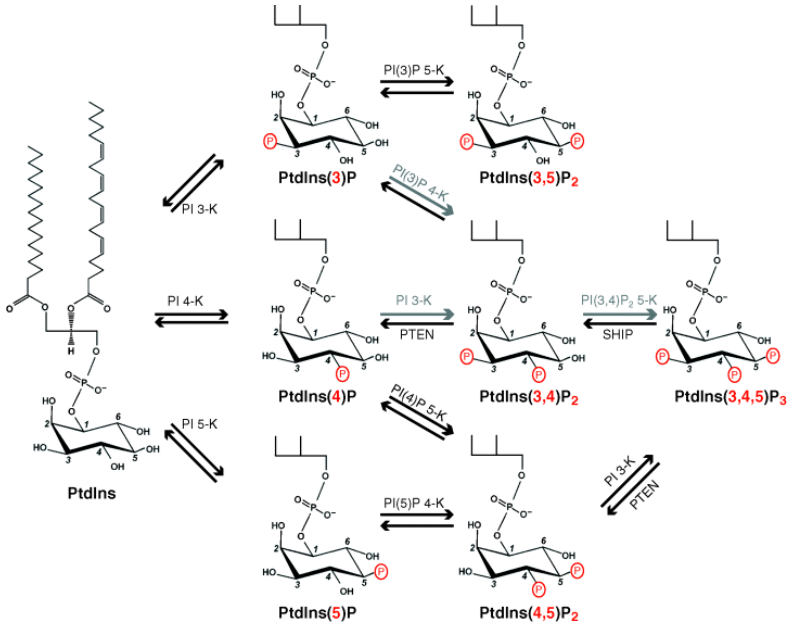

Figure 1.6: Biochemical network of phosphoinositide metabolism. *The kinases and phosphatases are named above and below the arrows, respectively. The pathways leading to the synthesis of PtdIns(3,4)P_2 (grey arrows) are controversial, and may depend on the cell type (Lemmon, 2003).*

There does not seem to be any requirement for the lipid moiety of phosphoinositides for the interactions with PH domains. The molecular basis for the stereospecific recognition of phosphorylated inositol head groups has been elucidated by several crystal structures of PH domain:ligand complexes (Baraldi et al., 1999; Ferguson et al., 2000; Ferguson et al., 1995; Lietzke et al., 2000; Thomas et al., 2002). In most of them, basic residues from the first two β-strands make crucial contacts to inositol ring and phosphate groups. In addition, there are ligand contacts from three variable loops (β1−β2, β3−β4, β6−β7) and the β7 strand of the protein. The region of the β1 and β2 strand contains a sequence motif ($KxGx_{6\text{-}13}N/TxKxRx\Phi$, where "x" is any amino acid and "Φ" is hydrophobic) that was first identified in a yeast assay that screened for PH domains that were specific for the products of PI-3K (Isakoff et al., 1998). While the motif is required for high affinity phosphoinositide binding, it is the three variable loops (β1−β2, β3−β4, β6−β7) that appear to determine ligand specificity. Hence these loops are sometimes referred to as "specificity determining regions" (SDRs).

It is still difficult if not impossible to predict the specificity of uncharacterised PH domains based on sequence alone. Thus, the phosphoinositide binding properties of pleckstrin C-PH which also contains the conserved motif on the β1 and β2 strands are determined experimentally in this thesis.

1.2 Nuclear magnetic resonance spectroscopy

Besides X-ray crystallography, nuclear magnetic resonance (NMR) spectroscopy is the only available technique that offers the possibility to study biological macromolecules at atomic resolution. The growing impact of NMR has been made possible by two major advances: the development of pulsed Fourier transform (FT) NMR (Ernst and Anderson, 1966) and the concept of multi-dimensional NMR spectroscopy (Jeener, 1971). Moreover, technical improvements, such as superconducting magnets with field strengths of currently up to 900 MHz and enhanced computer performance, have extended the applicability of NMR to larger systems and to more involved experimental and

computational schemes. Methods to produce isotopically (^{15}N and/or ^{13}C) enriched macromolecules and the successive development of heteronuclear multi-dimensional experiments were further advances, particularly for biomolecular NMR (Fesik and Zuiderweg, 1990). Most recently, access to long-range geometrical information for structure determination (residual dipolar couplings) (Tjandra and Bax, 1997; Tjandra et al., 1997; Tolman et al., 1995), as well as relaxation-optimised NMR experiments (TROSY) (Pervushin et al., 1997) of deuterated macromolecules have extended the scope of biomolecular NMR to large macromolecular complexes (Fiaux et al., 2002) and membrane proteins (Arora et al., 2001; Hwang et al., 2002).

The wealth of information that can be gained from NMR spectroscopy is based on the direct observation of NMR active nuclei. The most important applications of biomolecular NMR include structure determination, description of dynamical processes and investigation of intermolecular interactions.

In the following, structure determination by NMR is briefly described with special emphasis on multi-domain proteins. A glossary of technical terms and NMR concepts that are not explained in the text can be found in Appendix A.

1.2.1 Protein structure determination by NMR

Protein structure determination by NMR spectroscopy involves generally the following steps:

i. sample preparation
ii. data acquisition
iii. resonance assignment
iv. derivation of structural restraints
v. structure calculation and validation

The key to structural information is resonance assignment, a process that correlates the resonance frequencies of the signals in NMR spectra to the nuclei that give rise to them. For protein backbone assignment, triple-resonance experiments are recorded that correlate the amide backbone group (H^N and N) of each residue to the Cα and Cβ of its

own and the preceding residue (Sattler et al., 1999). By comparison of Cα and Cβ chemical shifts, neighbouring residues are identified. Chains of connected residues are formed and placed in the amino acid sequence of the protein by statistical analysis of chemical shift based on known ranges of chemical shifts for each amino acid type. After backbone assignment, the sidechain resonances are assigned by connecting all resonances in a sidechain to "anchor points" in the protein backbone, namely the Hα/Cα and H^N/N pairs. Sidechain assignment is not required for many applications of NMR, such as chemical shift perturbation experiments (binding site mapping) or relaxation analysis, because backbone assignment already provides information on a per-residue basis. However, for conventional structure determination, it is crucial since sidechain contacts in the hydrophobic core of a protein provide the majority of NMR-derived structural information (NOEs).

Once resonance assignment has been completed, the information content of NMR spectra becomes accessible. The ultimate result of spectral analysis is a set of estimated inter-nuclear distances and angles, called "restraints". The most important classes of restraints are (i) distance restraints derived from peaks in NOESY spectra ("NOEs") that correspond to proton-proton distances up to 5Å, (ii) dihedral angle restraints from J-couplings and secondary chemical shifts and (iii) projection angle restraints from residual dipolar couplings (RDCs). Another class of long-range distance restraints is derived from paramagnetic relaxation enhancement (PRE) as described in the sections below.

NMR derived restraints are used in a structure calculation together with geometric and non-bonded parameters (bond angles and lengths, Van-der-Waals radii etc.) that are known from small molecules. A large number of structures (an "ensemble") are computed in a simulated annealing molecular dynamics calculation. Comparison of the structures in the ensemble provides a measure of precision (how well the structure calculation has converged), whereas accuracy (structural quality) is assessed by different methods, such as the Ramachandran plot. In practice, resonance assignment, derivation of structural restraints and structure calculation/validation is an iterative process, in which more and more structural restraints are accumulated that drive an initial towards the final structural ensemble.

1.2.2 Structure determination of large and multi-domain proteins by NMR

Currently, the most important source of restraints is the nuclear Overhauser effect (NOE) which is exploited to measure distances between pairs of protons up to 5Å. For proteins larger than 20-25kDa, NOEs can no longer supply the bulk of information that is required to accurately calculate molecular structures, for the following reasons: complete ^{1}H resonance assignment becomes unattainable due to spectral crowding and reduced sensitivity of many experiments (Gardner and Kay, 1998). These are both direct consequences of increased molecular size. Deuteration in addition to $^{15}N/^{13}C$ labelling and optimised experimental schemes (Gardner and Kay, 1998; Pervushin et al., 1998; Pervushin et al., 1997) restore the sensitivity and improve the resolution of most experiments such that complete sequential backbone assignment is routinely achievable for medium sized proteins. Yet, assignment of sidechain protons, which are by definition replaced with ^{2}H, cannot be carried out with fully deuterated samples. The NOEs that remain in perdeuterated proteins, essentially only between amide protons, are sufficient to identify segments of secondary structure (α-helices, β-sheets), but usually not to define the relative position of theses elements to each other, although the use of very long mixing times may be an option to extend the range of the NOE up to 8Å (Koharudin et al., 2003). Selective labelling techniques that reintroduce a small degree of protonation (e.g. in methyl groups) enlarge the set of assignable protons that give rise to NOEs (Gardner et al., 1997; Goto et al., 1999; Rosen et al., 1996). In this way, the global fold of medium sized proteins can be determined, especially in combination with residual dipolar couplings (RDCs) (Mueller et al., 2000). RDCs by themselves are not sufficient to determine the global fold in most cases because they only provide rotational, but no translational information (i.e. only angles between bond vectors, but not their relative distance). However, RDCs are an excellent source of long-range structural information which is complementary to NOE or NOE-like data (Tjandra and Bax, 1997; Tolman et al., 1995). Since selective protonation in a deuterated background is extremely expensive, alternative strategies to obtain a satisfactorily large set of NOE-like distance restraints have to be developed.

Paramagnetic relaxation enhancement (PRE) is one such alternative. It defines distances between ^{1}H nuclei and a paramagnetic electron in the range of 10 to 25Å. Since only very

simple experiments need to be carried out to measure PRE, no special isotopic labelling schemes (except conventional ^{15}N and maybe in some cases ^{13}C labelling) are required. The size of the molecule is not inherently limiting, as long as backbone assignment is feasible. These characteristics theoretically allow PRE to be used to define distances between secondary structure elements in large proteins, between domains in multi-domain proteins and between individual components of molecular complexes. Since the information content of PRE data is "translational" (distances between atoms) it is complementary to RDCs which provide "rotational" information (angles between bond vectors and an external reference frame). The combination of PRE data with RDCs has a great potential for NMR structure determination of large systems.

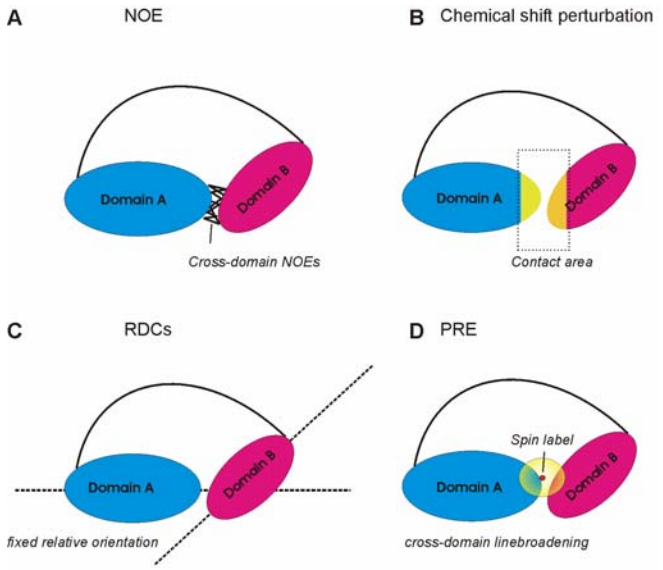

Figure 1.7: Different types of NMR-derived structural restraints for a hypothetical two-domain protein*. It is assumed that the structure of both domains is known. The linker between the two domains may adopt any conformation.* ***A:*** *NOEs. The inter-domain NOEs are represented as a network of short distances.* ***B:*** *Chemical shift perturbation. The contact area is represented in yellow.* ***C:*** *RDCs. The relative orientation of the two domains is fixed, as illustrated by two dotted axes.* ***D:*** *Paramagnetic relaxation enhancement (PRE). The paramagnetic group (spin-label) is represented as a red ball. The radius of PRE is shown as a yellow sphere.*

A multi-domain protein whereof all individual domain structures are known constitutes a special case of a large molecular system. Several NMR methods can be employed to obtain the relative position and orientation of two or more domains (Fig. 1.7). Inter-domain NOEs (Fig. 1.7A) provide the most accurate information but they have to be

sought like the proverbial needle in the haystack among a huge number of trivial intra-domain NOEs. Chemical shift perturbation (Fig. 1.7B) is often not conclusive enough because the data are too imprecise. By contrast RDCs (Fig. 1.7C) and PRE (Fig. 1.7D) caused by a paramagnetic spin-label provide relatively accurate information on domain-domain orientation and inter-domain distances, respectively. Thus, they are the methods of choice for the structure determination of multi-domain proteins.

1.2.3 Spin-labels

The reason why PRE is not widely applied to obtain long-range structural restraints is that it is quite difficult to obtain a paramagnetic sample of a protein. Metalloproteins are the exception: replacement of a diamagnetic metal ion (e.g. Zn^{2+}) with a paramagnetic one (Co^{2+}) is all that needs to be done. Accordingly, PRE has been employed extensively in structural studies of metalloproteins (Bertini et al., 2001).

For non-metal-binding proteins, a paramagnetic group has to be artificially attached to a macromolecule. Several methods have been established to connect extraneous groups or motifs to a protein that chelate a paramagnetic metal ion (Donaldson et al., 2001; Iwahara et al., 2003; Iwahara et al., 2004; Pintacuda et al., 2004). Alternatively, a stable organic paramagnetic compound, such as the proxyl group (Fig. 1.8), may serve as a "spin-label". The discipline of electron paramagnetic resonance (EPR) spectroscopy has pioneered the development of techniques that "spin-label" an otherwise diamagnetic protein via cysteine sidechains. Soon after, these methods were also applied in the NMR field (Kosen, 1989). Spin-labelling is easily achieved for proteins that contain a single accessible cysteine (Fig. 1.8). In the case of a cysteine-free protein, a cysteine residue can be introduced by site-directed mutagenesis which offers the possibility to produce several variants of a protein that are spin-labelled at different positions. Therefore "site-directed spin-labelling" is a powerful approach to probe the entire surface of a protein (Hubbell et al., 1998). Unfortunately, there are only few proteins which do not contain any (accessible) cysteine. If a protein already contains cysteines, it is necessary to first replace all accessible ones by mutagenesis – on the order of 1-2 cysteines per 100 residues. This initial step is the most time-consuming one, especially for a larger protein.

Nonetheless, it is feasible if optimised molecular biology methods are employed, as demonstrated in Chapter 4 of this thesis.

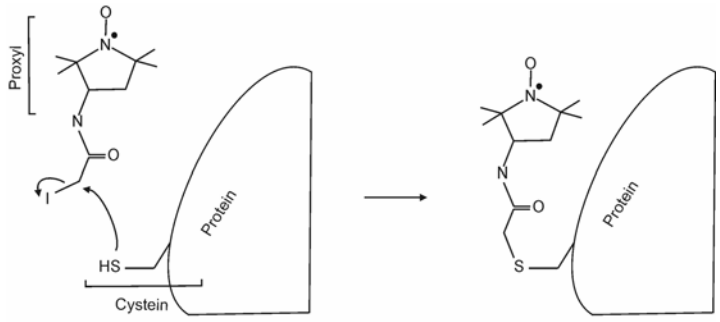

Figure 1.8: reaction of a spin-label reagent with a cysteine sidechain. *The reagent shown is 2-iodoacetamido-proxyl. The radical electron is located at the nitroxide group and illustrated as a black dot over the nitrogen.*

1.2.4 Theory of paramagnetic relaxation enhancement

Paramagnetic relaxation probes such as spin-labels increase the relaxation rates of the NMR resonances of nearby nuclei in a distance-dependent manner. The effect is caused by the dipolar interaction between the nuclear and the electron spin. PRE dominates over all other relaxation effects because of the large size of the electronic magnetic moment which is 572 times larger than for ^{1}H. For instance, all ^{1}H signals within a radius of 10Å to the radical electron of a spin-label are broadened beyond detection ("bleaching"). In the following, the equations describing PRE caused by a nitroxide spin-label are presented and different methods for measuring PRE and converting it into distance restraints are introduced.

The magnetic interaction of a free electron with a proton is described by the Solomon-Bloembergen equations (Kosen, 1989; Solomon and Bloembergen, 1956). The enhancement of the proton's longitudinal (R1) and transverse (R2) relaxation rates is given by:

$$\Delta R1 = 2K(3\tau_c/(1 + \omega_H^2\tau_c^2))/r^6 \qquad (1)$$

$$\Delta R2 = K(4\tau_c + 3\tau_c/(1 + \omega_H^2\tau_c^2))/r^6 \qquad (2)$$

where K is the constant 1.23 x 10^{-32} cm^6 s^{-2} for a nitroxide radical, *r* is the vector distance between the radical electron and the proton, τ_c is the correlation time for the electron-proton vector and ω_H is the Larmour frequency of the proton. Both equations are based on the assumption that the vector between the electron and the proton is free to undergo isotropic rotational diffusion and that its length *r* is fixed. The constant K is composed of the following physical constants:

$$K = 1/20 \times \gamma^2 g^2 \beta^2 \qquad (3)$$

where γ is the nuclear gyromagnetic ratio, *g* is the electronic g factor, and β is the Bohr magneton.

The correlation time of the electron-proton vector can be calculated from equation (1) and (2) if both $\Delta R1$ and $\Delta R2$ are accurately measured or if either $\Delta R1$ or $\Delta R2$ are accurately measured at two different field strengths. For calculating distances directly from a single measurement of either $\Delta R1$ or $\Delta R2$, it is convenient to make the approximation that the correlation time of the proton electron vector is equal to the global correlation time of the macromolecule (protein). For proteins studied in this thesis τ_c is in the range of 8-12ns. Since NMR is carried out at 600MHz (ω_H) the term $\omega_H^2 \tau_c^2 >> 1$ and equation (2) simplifies to

$$\Delta R2 = K \times 4\tau_c / r^6 \qquad (4)$$

$\Delta R2$ depends on the distance between proton and electron by the inverse of the sixth power of *r* ("r^{-6} dependence"). Therefore, ΔR will be heavily biased in favour of shorter distances when dynamically averaged, as is also true for the NOE which has the same r^{-6} dependence.

When equation (4) is solved for *r*, the following relationship is obtained:

$$r = (K \times 4\ \tau_c / \Delta R2)^{1/6} \qquad (5)$$

Since *r* depends on the sixth-root of τ_c, the estimate of *r* will be relative insensitive to errors in τ_c. If typical values for τ_c (around 10ns) and $\Delta R2$ (5-100Hz, (Gillespie and Shortle, 1997)) are substituted into equation (5), the range of *r* is between 10 and 25Å (see also Fig. 1.9A). Thus, spin-labels are a workable probe in distance ranges far beyond the NOE (<5Å).

There are several ways how $\Delta R1$ and $\Delta R2$ can be measured. The most accurate way is to extract $\Delta R1$ and $\Delta R2$ from proton relaxation measurements (Donaldson et al., 2001; Gaponenko et al., 2000; Gillespie and Shortle, 1997). R1 and R2 are measured on a paramagnetic and a reference sample. The difference between the two experiments is the paramagnetic relaxation enhancement:

$$\Delta R1 = R1_{PRE} - R1 \quad \text{and} \quad \Delta R2 = R2_{PRE} - R2 \qquad (6)$$

where R1 and R2 are the intrinsic relaxation rates and the subscript "PRE" denotes the apparent relaxation rates of the paramagnetic sample.

$\Delta R2$ can also be extracted from the reduction in NMR signal intensity that is caused by the paramagnetic probe, thereby avoiding the elaborate scheme of analysing relaxation experiments. During an NMR experiment like the 2D-^{1}H,^{15}N-HSQC paramagnetic relaxation enhancement is most efficient for the transverse relaxation rate (R2) of ^{1}H. Effects on the longitudinal relaxation rate (R1) are considered to be insignificant at the slow-tumbling limit ($w_H^2\tau_c^2 >> 1$) compared to effects on R2. The interaction of the radical electron with the heteronucleus (^{15}N) is also negligible, since the constant K scales with the square of the nuclear gyromagnetic ratio which is 19 times smaller for ^{15}N compared to ^{1}H (eq. 3).

The intensity of a signal in a 2D-^{1}H,^{15}N-HSQC experiment is attenuated by paramagnetic relaxation enhancement in two ways. First, transverse relaxation is active during the pulse sequence; therefore the intensity of the signal at the beginning of the acquisition period is scaled by the factor $e^{-R2\tau}$, where τ is the time during which proton magnetisation is transverse (potential relaxation differences between in-phase and antiphase ^{1}H relaxation are ignored). In the HSQC experiment, τ is equal to the length of two INEPT transfer

periods, therefore $\tau \approx 10$ms. The intensity of a signal in a reference experiment (I_0) and in an experiment with paramagnetic relaxation enhancement (I_{PRE}) at the end of the pulse sequence is given by:

$$I_0 \sim e^{-R2\tau} \text{ and } I_{PRE} \sim e^{-R2_{PRE}\tau} \quad (7)$$

Second, transverse relaxation during the acquisition period determines the linewidth and the maximum intensity of a signal in the direct dimension (^{1}H). For a Lorentzian line the intensity (maximal peak height at $\nu=\nu_0$) is proportional to 1/R2. Therefore:

$$I_0 \sim 1/R2 \text{ and } I_{PRE} \sim 1/R2_{PRE} \quad (8)$$

Combining eq. 7 and 8, the intensity ratio I_{PRE}/I_0 is given by:

$$I_{PRE}/I_0 = e^{-R2_{PRE}\tau} / R2_{PRE} / (e^{-R2\tau} / R2) \quad (9)$$

Substituting the expression for $R2_{PRE}$ (eq. 6) and rearranging:

$$I_{PRE}/I_0 = R2\, e^{-\Delta R2\tau} / (R2 + \Delta R2) \quad (10)$$

Battiste & Wagner directly approximate the intrinsic rate R2 from the lineshape of a signal in the reference spectrum. ΔR2 can then be estimated from eq. 10 (Battiste and Wagner, 2000). Likewise, Gillespie & Shortle obtain values for ΔR2 from simulations using a similar relationship and demonstrate that this method obtains comparable values to proton relaxation measurements (Gillespie and Shortle, 1997). ΔR2 is then substituted into eq. 5 to calculate distances which are used as restraints for a structure calculation.

As is evident from eq. 10, the reduction in peak intensity also depends on the intrinsic linewidth (~R2) of a signal, which may vary considerably between individual amide protons. For a given value of ΔR2, the reduction in I_{PRE}/I_0 is much greater the smaller R2 is. The relationship between distance *r versus* ΔR2 and I_{PRE}/I_0 is illustrated in Fig. 1.9.

The simulated curves are calculated from eq. 4 and 10, with τ_c=12ns and values of 62.5, 125 and 250Hz for R2 (black, red and green curve, respectively, in Fig. 1.9B). The values of τ_c=12ns and R2=125s^{-1} are representative for the 28kDa N-PH_DEP double-domain construct of pleckstrin. R2=62.5s^{-1} and R2=250 s^{-1} are shown to illustrate how a twofold decrease or increase in R2 (the approximate range of R2 for amide protons) influences I_{PRE}/I_0 . A near-linear relationship is obtained for all curves in Fig. 1.9B between 12 and 20Å. It is conceivable that an error of about 2Å in distance *r* is to be expected if an average instead of a measured value of R2 is used.

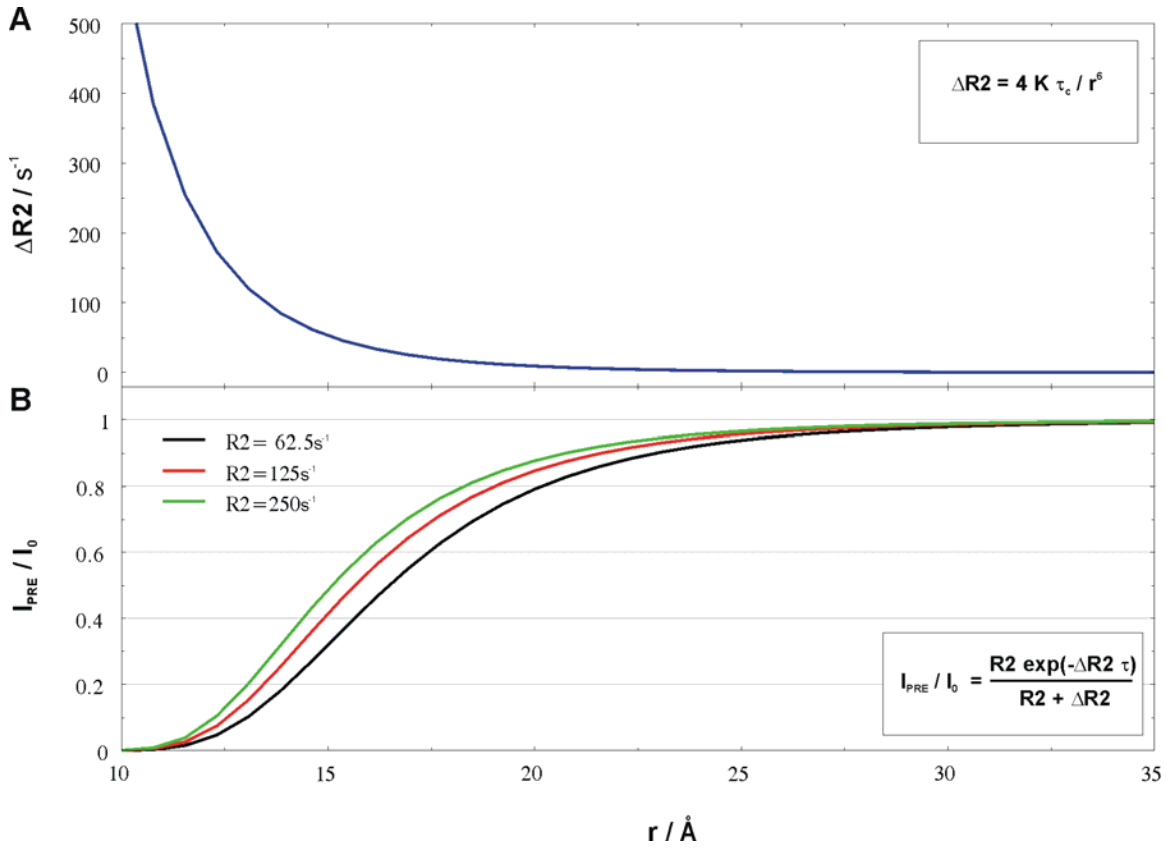

***Figure 1.9: Simulations of ΔR2 and I_{PRE}/I_0 versus distance r. A**: Values of ΔR2 are computed according to eq. 4 (inset), with τ_c=12ns. **B**: Values of I_{PRE}/I_0 are computed according to eq. 10 (inset), with values of ΔR2 calculated as for **A** and τ =10ms. Curves are shown for three different values of R2, representing an average value (125s^{-1}, red line) and values that are twice and half of it (62.5s^{-1} and 250s^{-1}, black and green line respectively).*

The disadvantage of using eq. 10 is precisely that intrinsic transverse relaxation rates have to be known for every signal in the spectrum. The approach to extract R2 from the lineshape of signals in the reference spectrum is unsatisfactory since the measurement of

relaxation rates is supposed to be replaced with the much simpler analysis of signal intensities. One way to avoid measuring or approximating intrinsic proton relaxation rates is to use an average R2 value. As discussed above this would introduce an additional error of up to ±2Å for a twofold difference in R2. A second alternative is to calibrate the signal intensity ratio directly against the distance *r*. Either, I_{PRE}/I_0 is calibrated against known distances in the molecule of interest (internal calibration) or if that is not possible, a standard curve based on known distances in a different molecule or on the theoretical relationship may be used (external calibration). Clearly, internal calibration is the method of choice because only in this way problems that are specific to the molecule can be identified reliably. A spin-labelled two-domain protein like N-PH_DEP for which both domain structures are known is ideally suited to carry out internal calibration: the distances from the paramagnetic electron to amide protons within the domain the spin-label is attached to are approximately known and can be used for the calibration of distances to the second domain. The procedure is very similar to the calibration of NOE-derived distances. In structure calculations of paramagnetic metalloproteins, PRE restraints are indeed treated like NOE restraints (Bertini et al., 2001). In chapter 4 of this thesis, the strategy to internally calibrate intensity ratios against distance is tested and implemented for the structure determination of two-domain proteins (chapter 4).

1.3 Outline of this thesis

In this thesis, the structural characterisation of the multi-domain protein pleckstrin is carried out in order to elucidate two aspects concerning its role in the platelet signalling network: a) the function of the yet-uncharacterised C-terminal PH domain and b) the overall architecture of the pleckstrin molecule and regulation thereof by phosphorylation. For this purpose, established NMR methods are applied, but also a novel strategy to obtain medium-resolution structures of multi-domain proteins is developed and put into practise. In addition to structural studies, the function of pleckstrin's PH domains is examined by biochemical methods.

In Chapter 2, the novel high-resolution structure of the C-terminal PH (C-PH) domain of human pleckstrin is presented. The phosphoinositide binding properties of C-PH are

analysed in detail by NMR and protein lipid overlay assays. The binding site on C-PH for the phosphoinositide ligand PtdIns(3,4)P_2 is mapped by chemical shift perturbation analysis. By comparison with known phosphoinositide:PH domain complex structures a model for the interaction between C-PH and its specific ligand is proposed. Furthermore, the biological implications of the specificity of C-PH for PtdIns(3,4)P_2 are discussed.

With the newly determined structure of C-PH and the already known structures of the N-terminal PH (N-PH) domain and the DEP domain of pleckstrin in hand, structural investigations of larger fragments of pleckstrin are initiated that aim to assemble the individual domain building blocks plus the connecting linker sequences into a "quaternary" structure. An intermediate step towards the understanding of the full-length three-domain protein is the study of double-domain constructs.

In Chapter 3, backbone resonance assignments of DEP_C-PH, the 230 amino acid C-terminal double-domain construct of pleckstrin, are reported. Chemical shifts and relaxation data of DEP_C-PH are compared to the isolated DEP and C-PH domains in order to identify regions where the two domains contact each other. The phosphoinositide binding properties of C-PH are also assessed in pleckstrin double-domain constructs and the full-length molecule. In this way, NMR and biochemical methods are combined to provide first insights into the molecular architecture of the C-terminal two-domain fragment of pleckstrin.

Since chemical shift and relaxation data analysis are not sufficient to obtain a medium-resolution structure of a pleckstrin double-domain construct, a different approach is taken in Chapter 4: paramagnetic relaxation enhancement by spin-labels is employed to obtain long-range restraints between two domains of pleckstrin. This method has not been previously applied to a protein of unknown structure and of similar size as pleckstrin; therefore methods for construct optimisation, data analysis and structure calculation are pioneered and made available for a wide range of applications. A preliminary structure of the N-PH_DEP double-domain construct is presented at the end of Chapter 4, showing the close association of N-PH and DEP and hinting at a possible mechanism of pleckstrin activation by PKC.

Chapter 5 summarises the most important results and conclusions of this thesis. Chapter 6 describes the experimental procedures that were employed in the course of this thesis. A

brief glossary of NMR spectroscopy is given in Appendix A instead of a more thorough description of NMR theory.

1.4 References

Abrams, C. S., Wu, H., Zhao, W., Belmonte, E., White, D., and Brass, L. F. (1995a). Pleckstrin inhibits phosphoinositide hydrolysis initiated by G-protein-coupled and growth factor receptors. A role for pleckstrin's PH domains. J Biol Chem *270*, 14485-14492.

Abrams, C. S., Zhang, J., Downes, C. P., Tang, X., Zhao, W., and Rittenhouse, S. E. (1996a). Phosphopleckstrin inhibits gbetagamma-activable platelet phosphatidylinositol-4,5-bisphosphate 3-kinase. J Biol Chem *271*, 25192-25197.

Abrams, C. S., Zhao, W., Belmonte, E., and Brass, L. F. (1995b). Protein kinase C regulates pleckstrin by phosphorylation of sites adjacent to the N-terminal pleckstrin homology domain. J Biol Chem *270*, 23317-23321.

Abrams, C. S., Zhao, W., and Brass, L. F. (1996b). A site of interaction between pleckstrin's PH domains and G beta gamma. Biochim Biophys Acta *1314*, 233-238.

al-Aoukaty, A., Rolstad, B., and Maghazachi, A. A. (1999). Recruitment of pleckstrin and phosphoinositide 3-kinase gamma into the cell membranes, and their association with G beta gamma after activation of NK cells with chemokines. J Immunol *162*, 3249-3255.

Arora, A., Abildgaard, F., Bushweller, J. H., and Tamm, L. K. (2001). Structure of outer membrane protein A transmembrane domain by NMR spectroscopy. Nat Struct Biol *8*, 334-338.

Auethavekiat, V., Abrams, C. S., and Majerus, P. W. (1997). Phosphorylation of platelet pleckstrin activates inositol polyphosphate 5-phosphatase I. J Biol Chem *272*, 1786-1790.

Balla, T., and Varnai, P. (2002). Visualizing Cellular Phosphoinositide Pools with GFP-Fused Protein-Modules. Science's STKE.

Baraldi, E., Carugo, K. D., Hyvonen, M., Surdo, P. L., Riley, A. M., Potter, B. V., O'Brien, R., Ladbury, J. E., and Saraste, M. (1999). Structure of the PH domain from Bruton's tyrosine kinase in complex with inositol 1,3,4,5-tetrakisphosphate. Structure Fold Des *7*, 449-460.

Battiste, J. L., and Wagner, G. (2000). Utilization of site-directed spin labeling and high-resolution heteronuclear nuclear magnetic resonance for global fold determination of large proteins with limited nuclear overhauser effect data. Biochemistry *39*, 5355-5365.

Bertini, I., Luchinat, C., and Piccioli, M. (2001). Paramagnetic probes in metalloproteins. Methods Enzymol *339*, 314-340.

Blomberg, N., Gabdoulline, R. R., Nilges, M., and Wade, R. C. (1999). Classification of protein sequences by homology modeling and quantitative analysis of electrostatic similarity. Proteins *37*, 379-387.

Boutros, M., Paricio, N., Strutt, D. I., and Mlodzik, M. (1998). Dishevelled activates JNK and discriminates between JNK pathways in planar polarity and wingless signaling. Cell *94*, 109-118.

Brumell, J. H., Craig, K. L., Ferguson, D., Tyers, M., and Grinstein, S. (1997). Phosphorylation and subcellular redistribution of pleckstrin in human neutrophils. J Immunol *158*, 4862-4871.

Brumell, J. H., Howard, J. C., Craig, K., Grinstein, S., Schreiber, A. D., and Tyers, M. (1999). Expression of the protein kinase C substrate pleckstrin in macrophages: association with phagosomal membranes. J Immunol *163*, 3388-3395.

Civera, C., Simon, B., Stier, G., Sattler, M., and Macias, M. J. (2004). Structure and Backbone Dynamics of the Human Pleckstrin DEP Domain. Biochemistry *(submitted)*.

Donaldson, L. W., Skrynnikov, N. R., Choy, W. Y., Muhandiram, D. R., Sarkar, B., Forman-Kay, J. D., and Kay, L. E. (2001). Structural characterization of proteins with an attached ATCUN motif by paramagnetic relaxation enhancement NMR spectroscopy. J Am Chem Soc *123*, 9843-9847.

Dowler, S., Currie, R. A., Campbell, D. G., Deak, M., Kular, G., Downes, C. P., and Alessi, D. R. (2000). Identification of pleckstrin-homology-domain-containing proteins with novel phosphoinositide-binding specificities. Biochem J *351*, 19-31.

Dowler, S., Currie, R. A., Downes, C. P., and Alessi, D. R. (1999). DAPP1: a dual adaptor for phosphotyrosine and 3-phosphoinositides. Biochem J *342 (Pt 1)*, 7-12.

Ernst, R. R., and Anderson, W. A. (1966). Application of Fourier Transform Spectroscopy to Magnetic Resonance. Rev Sci Instrum *37*, 93.

Ferguson, K. M., Kavran, J. M., Sankaran, V. G., Fournier, E., Isakoff, S. J., Skolnik, E. Y., and Lemmon, M. A. (2000). Structural basis for discrimination of 3-phosphoinositides by pleckstrin homology domains. Mol Cell *6*, 373-384.

Ferguson, K. M., Lemmon, M. A., Schlessinger, J., and Sigler, P. B. (1995). Structure of the high affinity complex of inositol trisphosphate with a phospholipase C pleckstrin homology domain. Cell *83*, 1037-1046.

Fesik, S. W., and Zuiderweg, E. R. (1990). Heteronuclear three-dimensional NMR spectroscopy of isotopically labelled biological macromolecules. Q Rev Biophys *23*, 97-131.

Fiaux, J., Bertelsen, E. B., Horwich, A. L., and Wuthrich, K. (2002). NMR analysis of a 900K GroEL GroES complex. Nature *418*, 207-211.

Frech, M., and Hemmings, B. A. (1998). PH domain of serine-threonine protein kinase B (RAC-PKB). Expression and binding assay for phosphoinositides and inositol phosphates. Methods Mol Biol *88*, 197-210.

Gaponenko, V., Howarth, J. W., Columbus, L., Gasmi-Seabrook, G., Yuan, J., Hubbell, W. L., and Rosevear, P. R. (2000). Protein global fold determination using site-directed spin and isotope labeling. Protein Sci *9*, 302-309.

Gardner, K. H., and Kay, L. E. (1998). The use of 2H, 13C, 15N multidimensional NMR to study the structure and dynamics of proteins. Annu Rev Biophys Biomol Struct *27*, 357-406.

Gardner, K. H., Rosen, M. K., and Kay, L. E. (1997). Global folds of highly deuterated, methyl-protonated proteins by multidimensional NMR. Biochemistry *36*, 1389-1401.

Gillespie, J. R., and Shortle, D. (1997). Characterization of long-range structure in the denatured state of staphylococcal nuclease. I. Paramagnetic relaxation enhancement by nitroxide spin labels. J Mol Biol *268*, 158-169.

Goto, N. K., Gardner, K. H., Mueller, G. A., Willis, R. C., and Kay, L. E. (1999). A robust and cost-effective method for the production of Val, Leu, Ile (delta 1) methyl-protonated 15N-, 13C-, 2H-labeled proteins. J Biomol NMR *13*, 369-374.

Harlan, J. E., Hajduk, P. J., Yoon, H. S., and Fesik, S. W. (1994). Pleckstrin homology domains bind to phosphatidylinositol-4,5-bisphosphate. Nature *371*, 168-170.

Harlan, J. E., Yoon, H. S., Hajduk, P. J., and Fesik, S. W. (1995). Structural characterization of the interaction between a pleckstrin homology domain and phosphatidylinositol 4,5-bisphosphate. Biochemistry *34*, 9859-9864.

Haslam, R. J., Koide, H. B., and Hemmings, B. A. (1993). Pleckstrin domain homology. Nature *363*, 309-310.

Hu, M. H., Bauman, E. M., Roll, R. L., Yeilding, N., and Abrams, C. S. (1999). Pleckstrin 2, a widely expressed paralog of pleckstrin involved in actin rearrangement. J Biol Chem *274*, 21515-21518.

Hubbell, W. L., Gross, A., Langen, R., and Lietzow, M. A. (1998). Recent advances in site-directed spin labeling of proteins. Curr Opin Struct Biol *8*, 649-656.

Hwang, P. M., Choy, W. Y., Lo, E. I., Chen, L., Forman-Kay, J. D., Raetz, C. R., Prive, G. G., Bishop, R. E., and Kay, L. E. (2002). Solution structure and dynamics of the outer membrane enzyme PagP by NMR. Proc Natl Acad Sci U S A *99*, 13560-13565.

Isakoff, S. J., Cardozo, T., Andreev, J., Li, Z., Ferguson, K. M., Abagyan, R., Lemmon, M. A., Aronheim, A., and Skolnik, E. Y. (1998). Identification and analysis of PH domain-containing targets of phosphatidylinositol 3-kinase using a novel in vivo assay in yeast. Embo J *17*, 5374-5387.

Iwahara, J., Anderson, D. E., Murphy, E. C., and Clore, G. M. (2003). EDTA-derivatized deoxythymidine as a tool for rapid determination of protein binding polarity to DNA by intermolecular paramagnetic relaxation enhancement. J Am Chem Soc *125*, 6634-6635.

Iwahara, J., Schwieters, C. D., and Clore, G. M. (2004). Ensemble approach for NMR structure refinement against (1)H paramagnetic relaxation enhancement data arising from a flexible paramagnetic group attached to a macromolecule. J Am Chem Soc *126*, 5879-5896.

Jeener, M. (1971). Unpublished lecture at the. Ampere International Summer School *Basko polje*, Yugoslavia.

Kavran, J. M., Klein, D. E., Lee, A., Falasca, M., Isakoff, S. J., Skolnik, E. Y., and Lemmon, M. A. (1998). Specificity and promiscuity in phosphoinositide binding by pleckstrin homology domains. J Biol Chem *273*, 30497-30508.

Koharudin, L. M., Bonvin, A. M., Kaptein, R., and Boelens, R. (2003). Use of very long-distance NOEs in a fully deuterated protein: an approach for rapid protein fold determination. J Magn Reson *163*, 228-235.

Kosen, P. A. (1989). Spin labeling of proteins. Methods Enzymol *177*, 86-121.

Lemmon, M. A. (2003). Phosphoinositide recognition domains. Traffic *4*, 201-213.

Lemmon, M. A., and Ferguson, K. M. (2001). Molecular determinants in pleckstrin homology domains that allow specific recognition of phosphoinositides. Biochem Soc Trans *29*, 377-384.

Lemmon, M. A., Ferguson, K. M., O'Brien, R., Sigler, P. B., and Schlessinger, J. (1995). Specific and high-affinity binding of inositol phosphates to an isolated pleckstrin homology domain. Proc Natl Acad Sci U S A *92*, 10472-10476.

Lietzke, S. E., Bose, S., Cronin, T., Klarlund, J., Chawla, A., Czech, M. P., and Lambright, D. G. (2000). Structural basis of 3-phosphoinositide recognition by pleckstrin homology domains. Mol Cell *6*, 385-394.

Liu, L., and Makowske, M. (1999). Phosphotyrosine protein of molecular mass 30 kDa binds specifically to the positively charged region of the pleckstrin N-terminal pleckstrin homology domain. Biochem J *342 (Pt 2)*, 423-430.

Lyons, R. M., and Atherton, R. M. (1979). Characterization of a platelet protein phosphorylated during the thrombin-induced release reaction. Biochemistry *18*, 544-552.

Ma, A. D., and Abrams, C. S. (1999). Pleckstrin induces cytoskeletal reorganization via a Rac-dependent pathway. J Biol Chem *274*, 28730-28735.

Ma, A. D., Brass, L. F., and Abrams, C. S. (1997). Pleckstrin associates with plasma membranes and induces the formation of membrane projections: requirements for phosphorylation and the NH2-terminal PH domain. J Cell Biol *136*, 1071-1079.

Macias, M. J., Musacchio, A., Ponstingl, H., Nilges, M., Saraste, M., and Oschkinat, H. (1994). Structure of the pleckstrin homology domain from beta-spectrin. Nature *369*, 675-677.

Majerus, P. W. (2001). In The molecular basis of blood disease (Stamatoyannopoulos, G., Majerus, P. W., Perlmutter, R.M., Varmus, H. eds.). Saunders *Philadelphia*, 764-780.

Mueller, G. A., Choy, W. Y., Yang, D., Forman-Kay, J. D., Venters, R. A., and Kay, L. E. (2000). Global folds of proteins with low densities of NOEs using residual dipolar couplings: application to the 370-residue maltodextrin-binding protein. J Mol Biol *300*, 197-212.

Offermanns, S. (2000). The role of heterotrimeric G proteins in platelet activation. Biol Chem *381*, 389-396.

Pervushin, K., Ono, A., Fernandez, C., Szyperski, T., Kainosho, M., and Wuthrich, K. (1998). NMR scalar couplings across Watson-Crick base pair hydrogen bonds in DNA observed by transverse relaxation-optimized spectroscopy. Proc Natl Acad Sci U S A *95*, 14147-14151.

Pervushin, K., Riek, R., Wider, G., and Wuthrich, K. (1997). Attenuated T2 relaxation by mutual cancellation of dipole-dipole coupling and chemical shift anisotropy indicates an avenue to NMR structures of very large biological macromolecules in solution. Proc Natl Acad Sci U S A *94*, 12366-12371.

Pintacuda, G., Moshref, A., Leonchiks, A., Sharipo, A., and Otting, G. (2004). Site-specific labelling with a metal chelator for protein-structure refinement. J Biomol NMR *29*, 351-361.

Roll, R. L., Bauman, E. M., Bennett, J. S., and Abrams, C. S. (2000). Phosphorylated pleckstrin induces cell spreading via an integrin-dependent pathway. J Cell Biol *150*, 1461-1466.

Rosen, M. K., Gardner, K. H., Willis, R. C., Parris, W. E., Pawson, T., and Kay, L. E. (1996). Selective methyl group protonation of perdeuterated proteins. J Mol Biol *263*, 627-636.

Sattler, M., Schleucher, J., and Griesing, C. (1999). Heteronuclear Multidimensional Experiments for the Structure Determination of Proteins employing Pulsed Field Gradients. Prog NMR Spectrosc *34*, 93-158.

Sloan, D. C., Wang, P., Bao, X., and Haslam, R. J. (2002). Translocation of pleckstrin requires its phosphorylation and newly formed ligands. Biochem Biophys Res Commun *293*, 640-646.

Solomon, I., and Bloembergen, N. J. (1956). N J Chem Phys *25*, 261-266.

Thomas, C. C., Deak, M., Alessi, D. R., and van Aalten, D. M. (2002). High-resolution structure of the pleckstrin homology domain of protein kinase b/akt bound to phosphatidylinositol (3,4,5)-trisphosphate. Curr Biol *12*, 1256-1262.

Tjandra, N., and Bax, A. (1997). Direct measurement of distances and angles in biomolecules by NMR in a dilute liquid crystalline medium. Science *278*, 1111-1114.

Tjandra, N., Omichinski, J. G., Gronenborn, A. M., Clore, G. M., and Bax, A. (1997). Use of dipolar 1H-15N and 1H-13C couplings in the structure determination of magnetically oriented macromolecules in solution. Nat Struct Biol *4*, 732-738.

Toker, A., Bachelot, C., Chen, C. S., Falck, J. R., Hartwig, J. H., Cantley, L. C., and Kovacsovics, T. J. (1995). Phosphorylation of the platelet p47 phosphoprotein is mediated by the lipid products of phosphoinositide 3-kinase. J Biol Chem *270*, 29525-29531.

Tolman, J. R., Flanagan, J. M., Kennedy, M. A., and Prestegard, J. H. (1995). Nuclear magnetic dipole interactions in field-oriented proteins: information for structure determination in solution. Proc Natl Acad Sci U S A *92*, 9279-9283.

Yoon, H. S., Hajduk, P. J., Petros, A. M., Olejniczak, E. T., Meadows, R. P., and Fesik, S. W. (1994). Solution structure of a pleckstrin-homology domain. Nature *369*, 672-675.